

Investigating triaxial electrical properties of ceramic composites for electroporcelain insulators

A.N.N. Dowuona^{a,d}, A.Yaya^{a,e,*}, E. Nyankson^a, J.K. Efavi^a, L.N.W. Damoah^a, D. Dodoo-Arhin^a, V. Apalangya^b, E. Annan^a, E.K. Tiburu^c, B. Onwona-Agyeman^a and B. Tomiczek^d

^aDepartment of Materials Science & Engineering, CBAS, University of Ghana, Legon, Ghana

^bDepartment of Food Process Engineering, CBAS, University of Ghana, Legon, Ghana.

^cDepartment of Biomedical Engineering, CBAS, University of Ghana, Legon, Ghana

^dInstitute of Engineering Materials and Biomaterials, Faculty of Mechanical Engineering, Silesian University of Technology, Gliwice, Poland

^eInstitut des Matériaux Jean Rouxel (IMN), UMR 6502, CNRS, Université de Nantes, 2 rue de la Houssinière, 44322 Nantes Cedex 3, France

Four porcelain composites comprising kaolin (27-37%), beach sand (20-24%), ball clay (13-18%) and feldspar (25-40%), were formulated and characterized using powder XRD, SEM and particle size distribution analysis in order to determine their potential for use as electroporcelain insulators. Chemical, mechanical and electrical properties were also evaluated. Each of the formed samples were compressed at 200 MPa and sintered at 1250 °C for 1 hour. Bending strength results of the porcelain bodies showed increase in bending strength with reduction in particle sizes. An increase in dielectric strength was found for samples with a higher felspar content. The XRD pattern for all the sintered samples showed the presence of quartz and mullite phases in the body at different intensities. Samples with lower particle sizes showed similar electrical and mechanical properties to commercially available electroporcelains albeit at a cheaper cost of production.

Key words: Ball milling, Particle sizes, Electroporcelains, SEM, XRD.

Introduction

Porcelains are a very important class of ceramic materials which at room temperature, have resistivity between $10^{12} \Omega$ - $10^{14} \Omega$ [1-2]. These are known to be composed of kaolin, feldspar and quartz crystal aggregates embedded in a glassy matrix [1]. In addition to their insulating properties, porcelains used for electroporcelain insulation are required to have low atomic mass, low defect concentration, high lattice stiffness, high purity with a minimum disorder and are usually covalent [1-5].

The individual phases have direct influence on the mechanical and dielectric strength of the formed body which is also hinged on concentration and microstructural characteristics [2, 6, 7]. Temperature and compositional differences are known to be the main driving forces which influence the microstructure and concentration of the phases present in these materials [5, 7]. Additionally, the mechanical behaviour of electroporcelains can be decisive in whether it is practically useable or not. The wide range of chemical and geographical compositions in the raw materials is also thought to influence it

mechanical strength.

Over the years, many studies have been conducted to improve properties such as; density, fracture toughness, and dielectric of ceramic materials which limit their use as out-door electrical materials. One of the earliest was the use of Aluminium Nitride as a reinforcement in ceramics [7]. This material has very high electrical resistivity and also minimal dielectric losses. Another work involved the improvement of ceramic properties that are fabrication method dependent [8]. For simple geometry, powder compaction is one of the conventional methods in ceramic composite fabrication [8, 9].

In order to optimise the electrical behaviour of a porcelain insulator, it is necessary to increase its resistivity as much as possible. In one of such works, zeolite was added in varying concentrations to porcelain [1]. It was then concluded from the study that, the resistivity of the porcelain-zeolite composite had much higher resistivity than the pure material. This resistivity increased with increasing zeolite concentration. Other studies were geared towards improving properties such as fracture toughness of ceramic materials, in which alumina ceramic composites was reinforced by adding graphene platelets, and this increased the flexural strength and fracture toughness by 30.75% and 27.20%, respectively [2].

*Corresponding author:
Tel : +233541835311
E-mail: ayaya@ug.edu.gh

In this work, we seek to identify the potential of different deposits in Ghana and harness them for the development of electroporcelain insulators that could withstand higher voltage without breakdown, using raw minerals from Ghana. The base mineral is kaolin which has been extensively characterized both locally due to its availability and low cost. Recent studies on kaolin have explored its use in composite reinforcement and for refractory bricks and porous filters [14], as well as for biomedical applications [9-13]. Two kaolin clay sources in southern Ghana, Assin-Fossu and Kumasi clays, have been investigated and characterized for application in electroporcelain insulator fabrication [15]. In the current study we extend this work to improve the base kaolin mechanical and electrical properties through the introduction of locally sourced composite fillers; beach sand, ball clay and feldspar, as well as exploring the effects of initial particle size and treatment on the resultant final porcelain ceramic. Tuning the kaolin properties in this way results in cheap, locally sourced and easily produced electroporcelains with properties comparable to current commercially available materials.

Experimental Procedures

Raw Materials

The raw materials that were used in the fabrication of the test specimen are ball clay from Mfensi in the Atwima Nwabiagya District in the Ashanti Region. Feldspar is mined from Ekrobadzi in the Mfantseman Municipality in the Central Region of Ghana. Kaolin from Aluku in the Ellembelle district of the Western Region of Ghana and quartz from Atuabo in the Ellembelle district in the Western Region of Ghana. The raw materials were located and excavated during the rainy season of July, 2016. Processing was done with tap water.

Sample preparations

The raw materials were collected from the deposits and dried in open air for 6 hours at a temperature of 30 °C and atmospheric humidity of 80%. The ball clay was initially placed into a gyratory to break down the lumps into smaller particles. The sample was then put into a pulverization machine, (puverisitte 5 ball milling machine, Fritsch, Germany) and ball milled at 400 revolutions per minute (rpm) for 15 minutes using a ball of mass, 500 g.

Similar procedures were repeated for the rest of samples (kaolin, feldspar and quartz). Magnetic bars were used to screen each powdered sample to remove iron fillings and then sieved through an aperture size of 0.5 mm.

The samples were put into a Turbula mixer and mixed for 15 minutes at a speed of 50 rpm. The mixing bowl was cleaned and dried after every material mix.

Table 1. Design of batch composition for the various samples.

Raw Materials	Aluku kaolin	Atuabo Sand	Mfensi Clay	Ekrobadzi Feldspar	Total
A (wt/wt %)	27	20	13	40	100
B (wt/wt %)	37	20	18	25	100

Table 2. Summary of samples and their respective ball milling conditions.

Sample	Raw Material Batch	Ball milling conditions
A-SB	A	155.85 g of ZrO ₂ media, 15 min. and 400 rpm
B-SB	B	
A-BB	A	500 g of ZrO ₂ media, 15 min. and 400 rpm
B-BB	B	

The batch composition for the mix is shown in table 1.

The amount of each material added is defined by a percentage of the total volume of the composition. The batch composition was mixed in a system schatz powder mixer (Turbula, Switzerland).

Each of the batch mixes, A and B were divided into two parts. One part was put in a 250 ml ball mill container with small milling balls (SB) made of zirconium oxide of mass 155.85 g with radius of 10 mm. The other part was put in a 500 ml ball mill container with big milling balls (BB) made of zirconium oxide of mass 500 g and a radius of 20 mm. Each was milled for 15 minutes at 400 rpm. A similar procedure was followed for batch mix B. Therefore both A and B had two different starting materials; one that was ball milled after the batch formulation using 155.85 g balls (named here as A-SB and B-SB for A and B respectively) and the other was ball milled after batch formulation using the 500 g balls (named here as A-BB and B-BB for A and B respectively). Table 2 summarizes the ball milling conditions for the various samples. All starting materials were screened with magnetic bars to remove iron fillings. Samples from each of the starting materials was taken and analyzed.

Characterisation

Test bodies were produced by weighing 8.0 g each of batch sample into a bowl. Clean water amounting to 6% of the mass of the sample was added to make a slurry. It was then uniformly stirred to ensure a homogenous mix. The preformed, with enough plasticity was put into the mold. The mold that was used to form the test bars was stainless steel body Sandvik Baildonit mold with a cavity dimensional capacity of 55 mm × 6 mm × 9.99 mm. The mold containing the green body was compressed by the Fontijne Grotnes hydraulic compression machine (Fontune Presses, United States) at 200 MPa, with a speed of 30 mm per minute and held for 1.5 minutes. The compressed specimens were dried in a furnace (Bego Miditherm 200MP, Germany) for 24 hours at 110 °C before cooling to room temperature. The specimen

were then sintered in the furnace at a rising temperature of 6 °C / min up to 1250 °C and held for 1 hr. The furnace containing the specimen was allowed to self-cool to a temperature of 200 °C and the specimen removed and cooled by air to room temperature.

The sintered samples were measured for shrinkage by determining the length of the samples before and after firing and expressing the difference as a percentage of the value before firing. The average value of the specimen for each composition will represent the lengthwise shrinkage.

A Zwick Roell Z220 Universal Testing machine was used to measure the bending strength of samples. A bending speed of 1 mm per minute was used to break the sample, which was 30 mm between two points. Thickness and width of the samples were measured afterwards. Also, modulus of rupture, the strain and the yield strength were measured. A minimum of five specimens were tested for each batch mix and the average recorded. The apparent density was determined by using the mass and volume measurements of fired sample.

Powder X-ray diffraction patterns of the samples were obtained using PAN analytical X'Pert PRO X-ray diffraction system using Co-K α radiation in the 2 θ range of 20-90 ° with a step size of 0.026 ° and a counting time of 15s per step. SEM images of powdered raw samples were observed using a SUPRA 35, ZEISS scanning

electron microscope. Particle size distribution analyzer Analysette 22 MicroTec plus, Fritsch, was used to analyse the particle sizes. Dielectric measurements were done using a high voltage breaking voltage test machine (Terco HV-9133, Sweden).

Results and Discussion

Table 3 shows the average apparent densities of the powdered mineral materials and batched samples A and B which were milled with either small ball (SB) or big ball (BB). There was no flow ability observed in the samples. The kaolin recorded the highest (0.802 g/cm³) apparent density and ball clay (0.561 g/cm³) with the lowest of the samples.

The particle size distribution curves for the raw mineral and batched samples are shown in Figs. 1-2 with the average mean diameters given in Table 4. The curve in Fig. 1 (a and c) shows a radial distribution function for kaolin and ball clay implying that, most of the particles sizes from these two minerals are of the same diameter which are much lower in particle sizes compare to feldspar and sand minerals in Fig. 1 (b and d) which shows much higher particle sizes with different particle size distributions. Ball clay with the lowest mean particle size of 14.53 μ m, means it has finer grains which invariably will give rise to higher

Table 3. Apparent densities of raw materials and batched samples.

	Aluku kaolin	Sand (Atuabo)	Ball clay (Mfensi)	Feldspar (Ekorbazde)	Sample A-BB	Sample A-SB	Sample B-BB	Sample B-SB
Apparent density (g/cm ³)	0.802	0.742	0.561	0.592	0.536	0.549	0.533	0.545

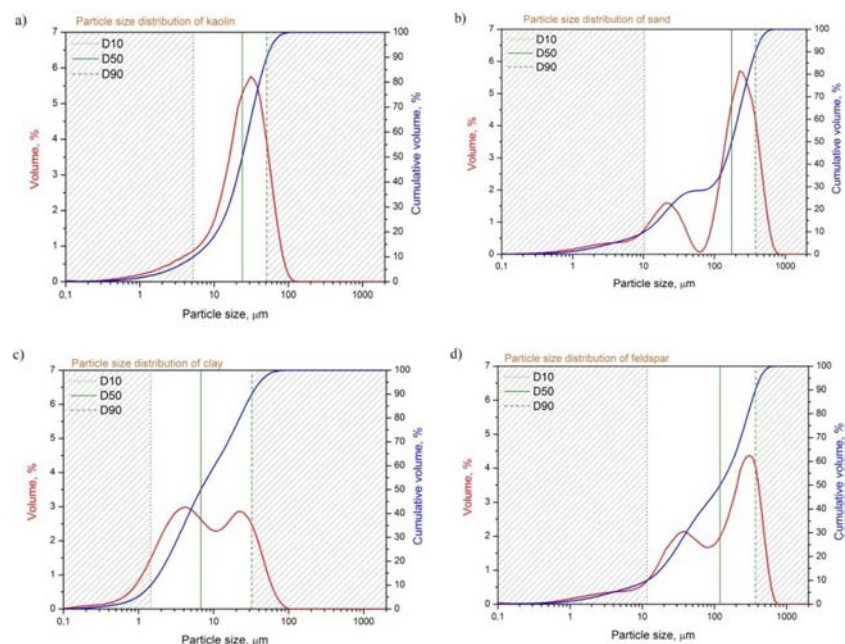


Fig. 1. Particle size distribution curves for; a) kaolin b) sand c) ball clay and d) feldspar.

plasticity, see Table 4. The distribution of particles is the principal cause for plasticity of clay materials [16]. The kaolin also has a uniform distribution of its particle sizes while the sand and feldspar show a non-uniform distribution (Fig. 1). Similarly, the distribution in cumulative volume of the batched samples is shown in Fig. 2, with their mean and mode values in Table 4. This shows that, the particles sizes are of different diameters in all the samples (Fig. 2), but it turns out that the mean value for sample B-BB was the least and sample A-SB with the highest value, see Table 4.

The mean values for the particle sizes of the milled materials represent the average size of the particles in the batch. The implications for this are that, particle sizes and distribution affect the vitrification and porosity of the sintered porcelain body. To confirm the particle sizes distribution for the raw minerals, SEM was used to characterize the morphology of the raw mineral samples in Fig. 3.

The SEM images show smaller particle sizes for the kaolin and ball clay, while sand and feldspar show relatively bigger particle sizes which agrees with the particle distribution curves for the raw minerals. EDS measurements gave the prevalence of the dominant elements that are characteristic of clay materials and other elements as previously reported in our study on

clay materials [15].

The X-ray powder diffraction of the investigated minerals is given below in Fig. 4. These patterns upon identification and matching of the peaks show that; in the kaolin, peaks with highest intensity and crystallographic (111) plane is quartz. Other peaks represented the intensities of muscovite, vermiculite and mica [17]; the pattern for sand shows the presence of quartz in the powder. Other minerals include calcite (c) and albite (a); that for ball clay contains quartz, muscovite (m), vermiculite and mica (M); feldspar contains quartz in the powder. Also present are microcline (Ml) and albite (a).

Having characterised and confirming the presence of the raw minerals in samples, we further discussed their mechanical characteristics in relation to the formulated batches. The average dimensions and density of samples A and B that were milled with small ball (SB) and big ball (BB) were recorded after machine pressing and drying from which the average percent shrinkage was estimated (after sintering the samples at 1250 °C) to be; A-BB (4.99%), A-SB (5.00%), B-BB (4.14%) and B-SB (4.43%), see Fig. 5.

The shrinkage percentage for the sintered porcelain bodies increases marginally with increase in mean particle size values for the batch composition (Fig.5).

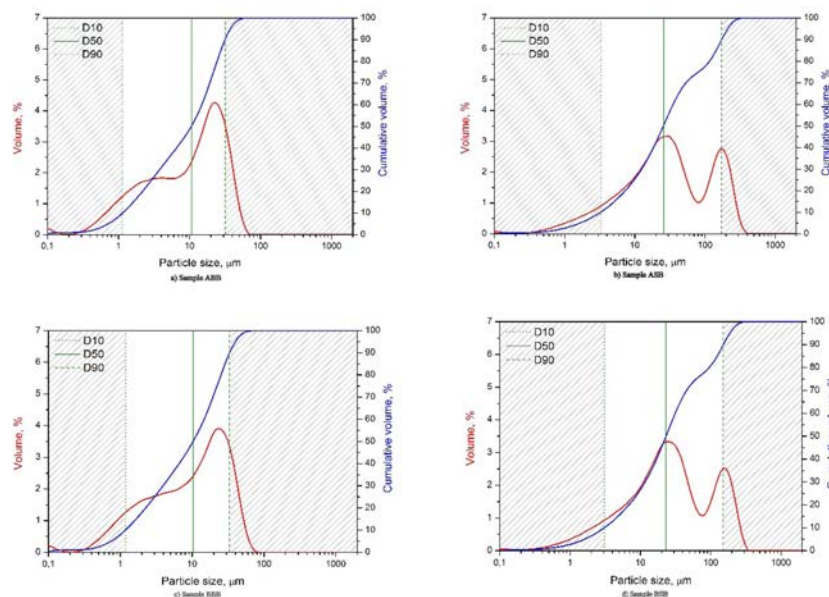


Fig. 2. Particle size distribution curves for milled; sample 'A' using a) 500 g, b) 155.85 g balls and Sample 'B', c) 500 g and d) 155.85 g balls.

Table 4. Particle size of minerals and ball milled samples A and B; with small ball milled (SB) and big ball milled (BB).

	kaolin	sand	clay	feldspar	A-BB	A-SB	B-BB	B-SB
d10 (μm)	5.24	10.20	1.45	11.61	1.14	3.27	1.176	3.07
d50 (μm)	23.93	175.55	6.78	119.46	10.59	25.54	10.31	23.12
d90 (μm)	51.41	380.00	32.31	369.38	31.65	173.44	33.29	151.65
Mean (μm)	26.86	188.59	13.52	166.82	14.46	67.42	14.93	59.28
Mode (μm)	27.02	190.44	14.53	167.82	15.01	68.22	15.12	60.22

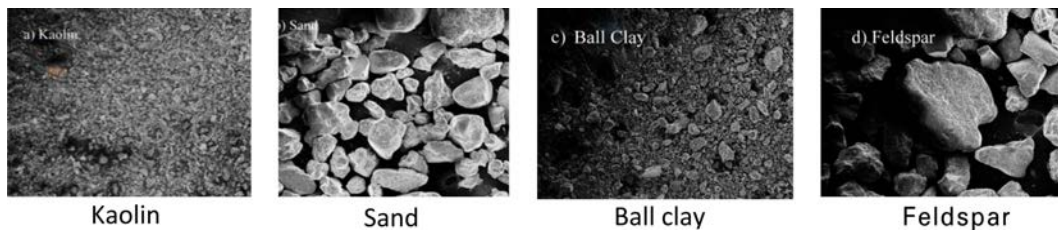


Fig. 3. SEM images of raw mineral samples with x100 magnification.

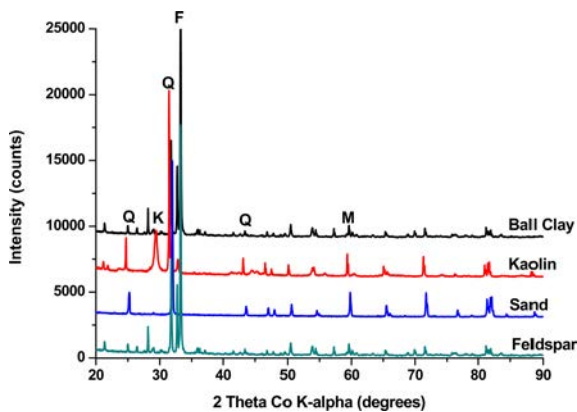


Fig. 4. XRD patterns for ball clay, kaolin, sand and feldspar.

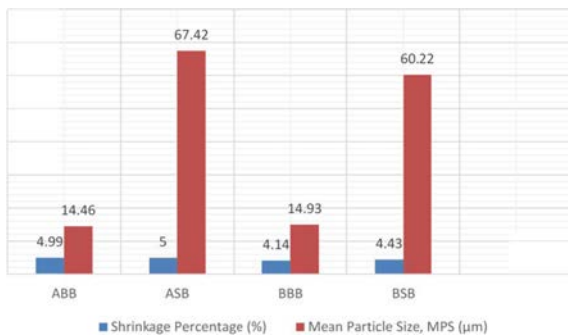


Fig. 5. Particle sizes of batch samples further milled compared with percent shrinkage of sintered bodies at 1250 °C.

The smaller the quartz grain sizes the greater the tendency to lose relative weight by over firing. Larger grains are known to cause cracks in the vitreous phase in contrast to fine quartz grains which melt very easily [18]. Also, bending strength test results are shown in Fig. 6. The bodies formed from samples that were further milled using small balls showed bending strength values less than 50% of the value of the same samples that were further milled using big balls.

The bending strength test on the single ball milled specimen 'A' formed bodies gave a value which was 54.25% less than that of specimen A-SB and 90.68% less for specimen A-BB. Similar trend was observed for samples B, B-BB and B-SB. As shown in Fig. 5, it implies that, in the fabrication of electrical porcelain bodies, it is particularly important to have fine particle size distribution in order to achieve the desired mechanical strength. Generally, firing temperature trend

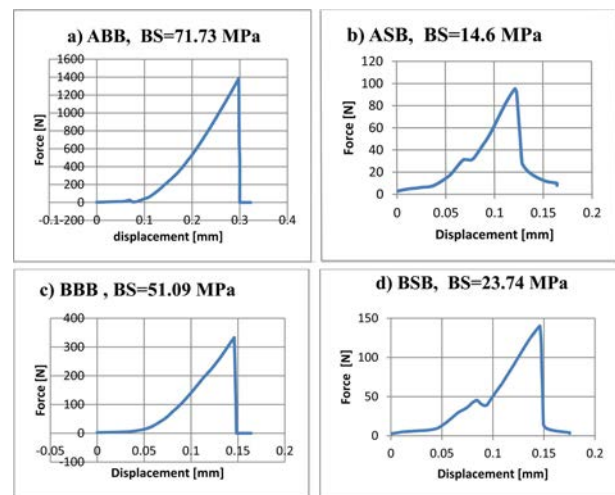


Fig. 6. Bending strength (BS) tests of fired (1250 °C) Samples ball milled using: 'A' a) 500 g, b) 155.85 g ball mill and 'B' c) 500 g, d) 155.85g ball mill.

shows that mullite content increases with temperature and also quartz grain size [18-20]. In order to test the insulation properties of formed porcelains bodies, their breakdown voltage was tested, see Table 5.

The breakdown voltage tests were done on samples A and B that have been further ball milled by small balls (A-SB and B-SB) and big balls (A-BB and B-BB) respectively. This was done to ascertain their suitability for electrical porcelain applications. The puncture test bodies for an average thickness of 5.13 mm porcelain test bodies are shown in Table 5. The test specimen A-BB showed the highest average breakdown voltage of 53.4 kV with breakdown strength of 10.45 kV/mm. This is indeed promising for future developments coupled with its bending strength of 71 MPa which compares to the standard value for pin type electrical porcelain insulator. The breakdown voltage test was carried out at room temperature.

The bending strength of the sintered bodies measured against the particle size mean values of the batch samples are shown in Fig. 7. This show that bending strength for the same batch composition increases with smaller particle size.

Conclusions

Electrical porcelain insulator bodies were fabricated using varying amounts of kaolin, sand, clay and

Table 5. Dielectric strength (DS) tests of samples (A & B) further ball milled by small balls (SB) and big balls (BB), sintered at 1250 °C. V_R = regulated voltage, V_B = breakdown voltage, I_B = breakdown current.

A-BB, 1250 °C DS = 10.45 KV/mm			A-SB, 1250 °C DS = 2.45 KV/mm		
V_R (V)	V_B (KV)	I_B (A)	V_R (V)	V_B (KV)	I_B (A)
0	0.1	0.2	0	0.1	0.2
7	4.9	0.1	3	2	0.2
13	8.6	0	9	6.2	0.1
17	53.4	0.2	14	9.3	0
			19	12.5	0.2

B-BB, 1250 °C DS = 3.69 KV/mm			B-SB, 1250 °C DS = 2.68 KV/mm		
V_R (V)	V_B (KV)	I_B (A)	V_R (V)	V_B (KV)	I_B (A)
0	0.2	0.2	0	0.2	0.2
5	3.8	0.1	5	3.8	0.1
11	7.4	0	11	7.7	0
16	10.5	0	18	12	0.1
18	18.9	0.2	24	13.7	0.2

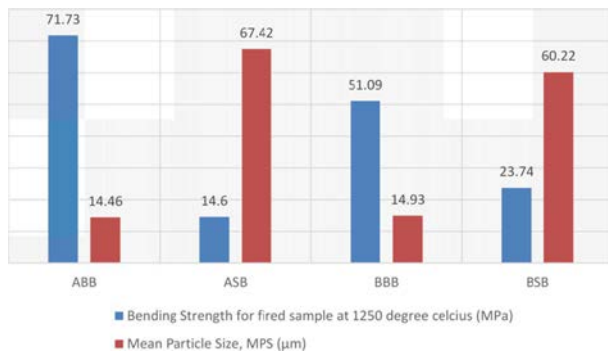


Fig. 7. Bending strength variations with particle sizes of Ball milled batch samples.

feldspar. Bending strength and dielectric strength of the formed materials were also evaluated. However, a wide variation in bending strength values was observed which may be due to the different amounts of composition in the raw minerals. Samples with a higher clay content showed higher dielectric strength. Sample A with a clay and kaolin content of 40%, and high feldspar content of 40%,

was found to be promising for the fabrication of pin type electrical insulations which meets international standards.

Acknowledgments

A.Y acknowledges support from the University of Ghana Building a New Generation of Academics in Africa (BANGA-Africa) Project, with funding from the Carnegie Corporation of New York.

References

1. J. Liu, H. Yan, M. J. Reece, and K. Jiang, *J. Eur. Ceram. Soc.* 32[16] (2012) 4185-4193.
2. J. Liu, H. Yan, and K. Jiang, *Ceram. Int.* 39[6] (2013) 6215-6221.
3. M.R. Winter and D.R. Clarke, *J. Am. Ceram. Soc.* 90[2] (2007) 533-540.
4. V.G. Sukumaran and N. Bharadwaj, *Trends Biomater. Artif. Organs* 20[1] (2006) 7-11.
5. A.S. Demirkiran, R. Artir, and E. Avci, *Ceram. Int.* 36[3] (2010) 917-921.
6. P.W. Olupot, S. Jonsson, and J.K. Byaruhanga, *Ceramics International* 36[4] (2010) 1455-61.
7. W. Werdecker and F. Aldinger, *IEEE Trans. Components, Hybrids, Manuf. Technol.* 7[4] (1984) 399-404.
8. I. Shishkovsky, I. Yadroitsev, P. Bertrand, and I. Smurov, *Appl. Surf. Sci.* 254[4] (2007) 966-970.
9. D. Obada, D.D. Arhin, M. Dauda, F. Anafi, A. Ahmed, and O. Ajayi, *Result Phys.* 7 (2017) 3838-3846.
10. D.E. Anderson et al., *Sensors* 17 (2017) 1831.
11. E. Tiburu, H. Fleischer, E. Aidoo, A. Salifu, B. Asimeng, and H. Zhou, *J. Biomimetics, Biomater. Biomed. Eng.* 28 (2016) 66-77.
12. E. Tiburu et al., *J. Biomater. Tissue Eng.* 7 (2017) 544-555.
13. E. Tiburu et al., *J. Nano Res.* 48 (2017) 156-170.
14. K. Efavi, L.D. Johnson, D.Y. Bensah, D.D. Arhin, and D. Tetteh., *Applied Clay Science* 65-66 (2012) 31-36.
15. A. Yaya, E. Tiburu, M.E Vickers, J.K Efavi, B. Onwona-Agyeman, and K.M Knowles, *Appl. Clay Sci.* (2017) 125-130.
16. C. Nkoumbou, A. Njoya, D. Njoya, C. Grosbois, D. Njopwouo, J. Yvon, and F. Martin, *Applied Clay Science* 43[1] (2009) 118-24.
17. J.W. Gruner, *Krist. Krist.* 83 (1977) 75-88.
18. O.I. Ece and Z. Nakagawa, *Ceram. Int.* 28 (2002) 131-140.
19. W.M Carty, and U. Senapati, *Journal of the American Ceramic Society* 81[1] (1998) 3-20.
20. J.M. Cases, P. Cunin, Y. Grillet, C. Poinsignon, and J. Yvon, *Clay Minerals* 21[1] (1986) 55-68.